# An analysis of the efficiency of Coanda - NOTAR anti-torque systems for small helicopters

*Anniversary Session **"Centennial celebration of the first jet aircraft invented by Henri Coanda"**, organized by INCAS, COMOTI and Henri Coanda Association, 14 December 2010, Bucharest, Romania*

Ionică CÎRCIU*, Mircea BOŞCOIANU*

*Corresponding author
"Henri Coanda" Air Force Academy, Braşov, Romania
circiuionica@yahoo.co.uk, boscoianu_mircea@yahoo.co.uk
DOI: 10.13111/2066-8201.2010.2.4.12

***Abstract:*** *The use of jet thrust for anti-torque for monorotor small helicopters is based on the circulation control concept, which result in a distributed side force along the entire tail boom assembly. High velocity jets of air from a pressurized tail boom is blown tangential to the surface out of narrow slots that run lengthwise on the side of the tail boom. In combination with the downstream velocity produced by the main rotor, Coanda jets cause the flow to remain attached to the tail boom surface. The anti-torque NOTAR system is in fact the result of Coanda effect and the interest is to analyze the efficiency of replacing the tail rotor on a small monorotor helicopter.*

*Keywords**:** Coanda effect, NOTAR, slot, attached jet, jet thruster*

## 1. COANDA EFFECT AERIAL VEHICLES

Coanda Effect is a classic phenomenon in fluid mechanics and one of the fundamental discoveries of the Romanian inventor Henri Marie Coanda (1886 - 1972). Henri Coanda was a Romanian inventor, aerodynamics pioneer and the designer and the builder of the world's first jet powered aircraft, the Coandă-1910, a revolutionary plane of the beginning of the 20th century.

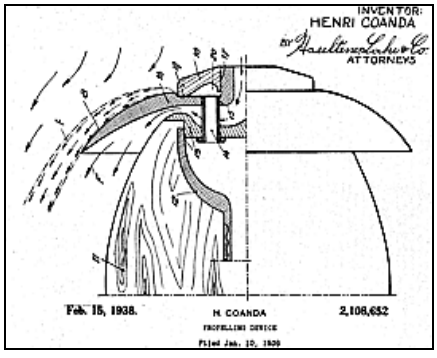


Fig. 1 Henri Coanda propelling device 0

As a natural phenomenon, Coanda effect describes the tendency of a fluid jet to be attracted to a nearby surface (flaps or airfoils), consecutively its profile being characterized by a significant asymmetry (Fig. 1).

In free surroundings, a jet of fluid entrains and mixes with its surroundings as it flows away from a nozzle. When a surface or another stream is placed close to the jet, this restricts the entrained air flow from surroundings into that region. As flow accelerates trying to

equalize the momentum transfer, a loss of pressure results across the jet and the jet is deflected closer to the surface, up to attaching to it.

Coanda's legacy was valued by researchers from many countries, mostly by developments and patents on Unmanned Aerial Vehicles (UAVs). We should also mention that the first design of a Coanda UAV was created in 1932 **0**, by the Romanian inventor Henri Marie Coanda.

After 2000, using mainly the Coanda effect, individual inventors as Robert Collins 0 and Geoffrey Hatton **0**, or companies as GFS Projects Ltd. and AESIR Ltd. (both from UK) and also a Romanian academic consortium, through MEDIAS project **0**, developed what we may consider a new class of aerial vehicles, the Coanda UAVs.

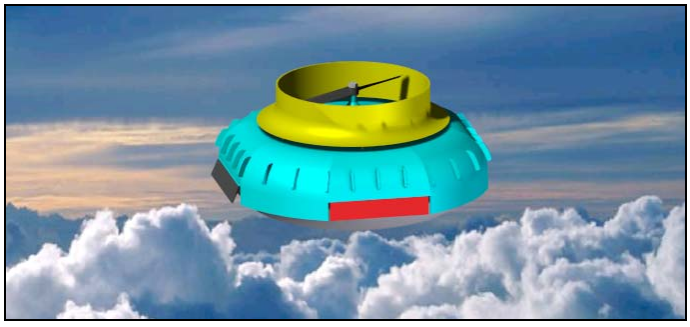

Fig. 2 MEDIAS-UAV (2009) **0**

In aeronautics, this effect is used today primarily in helicopters that have no tail rotors, as in NOTAR system **0**.NOTAR is the name of an anti-torque system which replaces the use of a tail rotor on a helicopter. It was developed by McDonnell Douglas Helicopter Systems and the name is an acronym derived from **NO TA**il **R**otor.

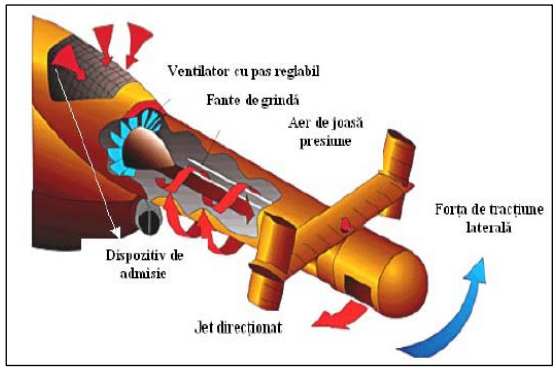


Fig. 3 The movement of air through the NOTAR system **0**

NOTAR uses a fan inside the tailboom to force a high volume of low-pressure air, to exit through two longitudinal slots and create a boundary layer flow of air along the tailboom utilizing the Coanda effect.

The boundary layer driven by Coanda effect changes the direction of airflow around the tailboom, thus creating a significant thrust on the fuselage. This airflow thrust is opposing to the motion imparted by the torque effect of the main rotor. Directional yaw control is gained through a vented, rotating drum at the end of the tailboom, called the jet thruster. **0**

## 2. A GLOBAL ANALYSIS OF THE MIXING PROCESS IN THE AIR EJECTOR

When studying the Coanda effect along the side of a curved wall, it is possible to notice the following aspects (Fig. 3.)

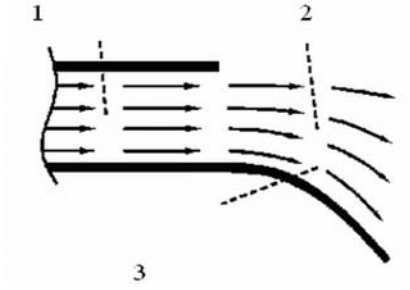


Fig. 4 Coanda effect (2D)

1. The depressurized zone (3) has as effects:
   - Flow acceleration upstream in the slot (1), without increasing upstream pressure or temperature,
   - Displacement of the local fluid.
2. Also, detaching and re-attaching is characterized by hysteresis (i. e. the reattaching occurs at smaller angles than the detaching).
3. The global stream that results from the mixing between the main flow and the displaced one is adherent to the wall and is characterized by a lower temperature than the initial one.

Let a Coanda ejector with non uniform and variable speed distribution. In the D exit section, the static pressure $p_D$ equals the environment pressure $p_H$. The power transferred to th fluid in D section is:

$$P_0 = \eta P_D = \int_{A_D} \rho_H V_D(y)\left(i_D^* - i_H^*\right) dA_D = \frac{\rho_H V^3{}_{MD} A_D \chi_{3D}}{2} \quad (1)$$

The absorption section, marked with (**h-h**), through which the inflow only advances, may be described as having the property that the total enthalpy $i^*$ of the inflow is the equal with that of the environment, $i_H^*$ .

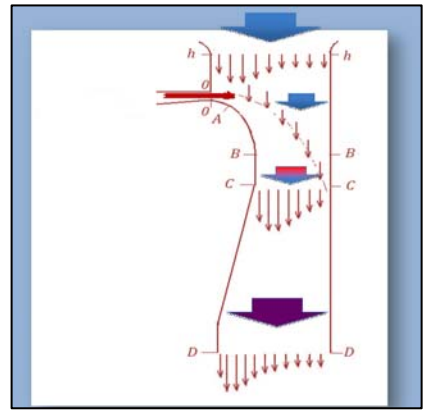


Fig. 5 Coanda ejector with: non uniform speed distribution

The place around **A** is considered to be the longitudinal spot from the tailboom, where the loss of pressure of the flow is maximal. Section **B-B** shows the end of the Coanda profile (line **OAB**).

Section **C-C** is where the absorption section ends and the mixing region extends to both walls. **D-D** is the exit section from the air ejector and is characterized by the fact that the static pressure is equal with that of the environment static pressure $p_H$.

The area **h-0-C-B-h** is considered to be the absorption area, where the total enthalpy, $i^*$ of the flow is: $i^* = i_H^*$ .

Area **0-ABC-C-0** is considered to be that of the junction where the both flows are mixing, where the whole generated flow is received through the permeable surface **C-0**.

Area **C-D-D-C** is the area of acquiring uniformity for the aero thermo gasodynamic parameters in section **C-C** and it usually has a divergent form, which favourably contributes to the efficiency of the air ejector.

Its existence leads to the increase of the generated flow, but it doesn't necessarily mean an increase of the propulsion force.

The research on the force increase will have to take into consideration the entire geometry of the air ejector.

The known factors are:

- Geometry of the air ejector in its sections (**Ah, A0, AB=AC, AD**),
- Fuel conditions in the slot ( $p^*, p_0$ ),
- Environmental conditions ( $p_H, \rho_H, i_H^*$ ).

Also, for this global analysis of the mixture in the air ejector, the values of the energetic performance ( $\eta_C, \eta_D$ ) on sections **00-CC**, **00-DD**, are considered to be known **[10]**.

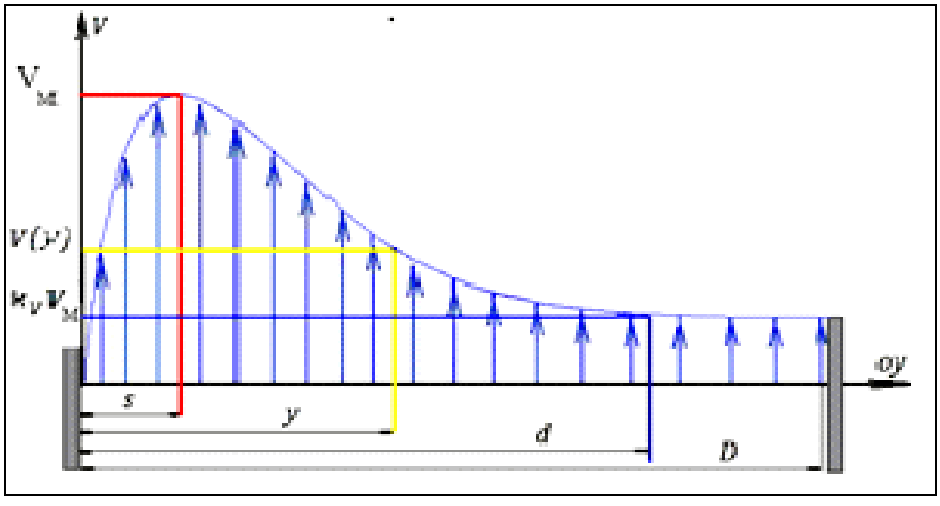


Fig. 6 Speed distribution across a section

In Fig.6 it is presented the distribution of the speed in a section of the Coanda air ejector, having two different regions, an asymmetrical one (*width=d*) and a uniform one (*width*=D-d), where *s* is the length of the boundary layer at the wall.

## 3. COANDA EFFECT STUDIED THROUGH COMPUTER ASSISTED FLOW MODELING

Coanda Effect Small Appliance is an experimental validation of using Coanda effect on the helicopter tailboom.


Fig.7 Experimental device: 1-NOTAR helicopter blades carbon fiber, 2 -hub pitch, 3-structure helicopter fiberglass,
4-Coanda slots, 5-device measuring dynamometer force F, 6-tool kit with, 7-measuring and control equipment 8-instruments for making measurements (timer, dynamometers, Anemometers electronic, mechanical comparator, roulette), 9 - dual source DC power, 10-stabilized power source and electronic oscilloscope.

A helicopter structure consists of two main components: a cabin and a tailboom of composite materials (glass and carbon fibre).In the Fig.7 may be seen the hub pitch and the blades of carbon fibre. This experimental model aims to highlight the Coanda effect and to measure the performance of propulsion. With this purpose in mind, the beam parameters were gradually modified, seeking to acquire a lateral force ***F*** as big as possible. The experimental device will show the fluid flow along the tailboom. This was simulated on a Coanda profile optimally adjustable, depending on the flows data load-bearing rotor, the intubated fan from the tailboom, and the location and geometry of the slot.

This optimization allows the suppression of the anti-torque rotor, thus eliminating its disadvantages. This leads us to benefit from a new favourable arrangement for creating higher lateral forces with lower energy consumption, compared to those data used in basic formulas describing the efficiency of the helicopters. In order to model the Coanda effect onto the flow from the helicopter tailboom, computer simulation was made using Solid Works 2007 software; the theoretical results we obtained may be seen in the following pictures, tables and diagrams (Fig. , Fig.  and Fig.10).

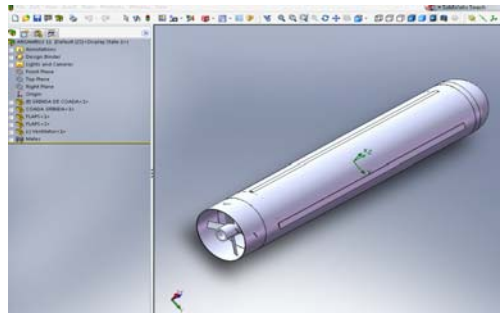

Fig. 8 3D model of the helicopter tailboom

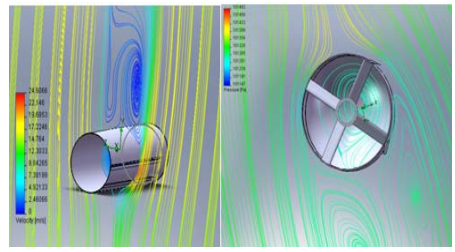

Fig. 9 A 3D view of Coanda effect flow through tailboom

This optimization allows the replacement of the rotor anti-torque eliminating its disadvantages and lead to the advantage given to obtain high lateral forces (maximum) with low energy consumption, which is found in formulas elements performance helicopters.

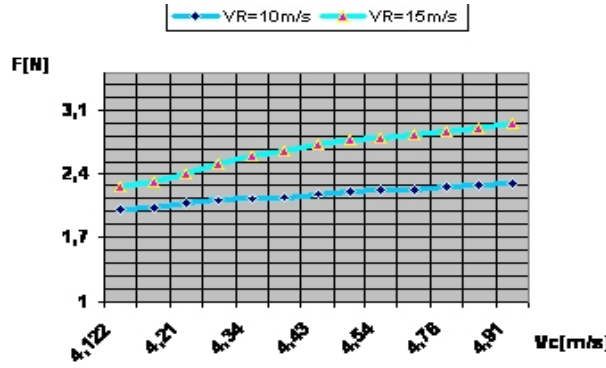


Fig. 10 The lateral force ***F***, depending on the speed $V_c$ ,
having a constant main rotor speed of $V_R$=15m/s, respectively $V_R$=10m/s.

Results from the experimental device with dimensions in table 1.

Table 1 The analysis of thye experimental results for a Coanda device with the following dimensions:length l = 30cm gap width = 2 mm and up blades p = $4^0$

| Nr. crt | $P$ | $p$ | $P_c$ | $V_{GC}$ | | $V_f$ | $V_R$ | $Q_R$ | $Q_{gc}$ | $2Q_f$ | $E_{fc}$ | F |
|---|---|---|---|---|---|---|---|---|---|---|---|---|
| UM | [W] | [$\theta_p$ $^0$] | [W] | Km/h | [m/s] | [m/s] | [m/s] | [$m^3$/s] | [$m^3$/s] | [$m^3$/s] | [N/W] | [N] |
| 1 | 70 | 4 | 6 | 19,4 | 5,30 | 5,74 | 7,22 | 8,161 | 4,242 | 0,00688 | 0,0783 | 0,47 |
| | | | 7,2 | 21,6 | 6,00 | 5,93 | | | 4,804 | 0,00710 | 0,0708 | 0,51 |
| 2 | | | 8,4 | 25,3 | 7,02 | 7,24 | | | 5,621 | 0,00868 | 0,0678 | 0,57 |
| | | | 9,6 | 28,3 | 7,86 | 7,35 | | | 6,294 | 0,00882 | 0,0666 | 0,64 |
| 3 | | | 10,6 | 30,8 | 8,55 | 8,65 | | | 6,846 | 0,01038 | 0,0660 | 0,70 |
| | | | 12 | 33,4 | 9,27 | 9,35 | | | 7,420 | 0,01122 | 0,0658 | 0,79 |
| 4 | 95 | | 6 | 19,4 | 5,30 | 5,91 | 8,31 | 9,393 | 4,242 | 0,00709 | 0,0950 | 0,57 |
| | | | 7,2 | 21,6 | 6,00 | 6,22 | | | 4,804 | 0,00746 | 0,0916 | 0,66 |
| 5 | | | 8,4 | 25,3 | 7,02 | 7,44 | | | 5,621 | 0,00892 | 0,0904 | 0,76 |
| | | | 9,6 | 28,3 | 7,86 | 8,12 | | | 6,294 | 0,00974 | 0,0875 | 0,84 |
| 6 | | | 10,6 | 30,8 | 8,55 | 8,89 | | | 6,846 | 0,01066 | 0,0896 | 0,95 |
| | | | 12 | 33,4 | 9,27 | 9,38 | | | 7,420 | 0,01125 | 0,0875 | 1,05 |
| 7 | 145 | | 6 | 19,4 | 5,30 | 5,98 | 9,56 | 10,806 | 4,242 | 0,00717 | 0,1133 | 0,68 |
| | | | 7,2 | 21,6 | 6,00 | 6,37 | | | 4,804 | 0,00764 | 0,1083 | 0,78 |
| 8 | | | 8,4 | 25,3 | 7,02 | 7,88 | | | 5,621 | 0,00945 | 0,1047 | 0,88 |
| | | | 9,6 | 28,3 | 7,86 | 8,39 | | | 6,294 | 0,01006 | 0,1041 | 1,00 |
| 9 | | | 10,6 | 30,8 | 8,55 | 9,12 | | | 6,846 | 0,01094 | 0,1037 | 1,10 |
| | | | 12 | 33,4 | 9,27 | 9,43 | | | 7,420 | 0,01131 | 0,1033 | 1,24 |

Interpretation of results was performed in graphical form as follows: A first step is to highlight the evolution of lateral force F due to Coanda effect depending on the power consumed by the rotor bearing the six-power variation of the fan beam intubated in the tail, was added to this step change blades with three values.

Figure 11 highlights the changes in lateral force due to Coanda effect to adjustments of power tools (three values: P = 70 [W], 95 [W], 125 [W]) applied to the rotor portal, maintaining constant width = 2mm to slot the same value of step blades $p = 4^0$.

For each amount of useful power applied to the rotor bearing was varied six-speed adjustable fan $P_C$ Power intubated in the beam tail.

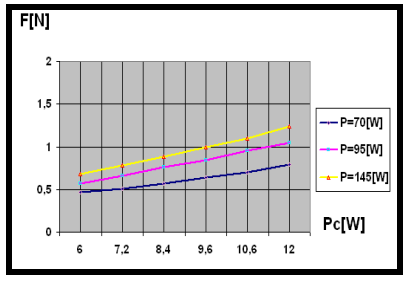


Fig.11 Variation lateral force F due to Coanda effect to maintain constant: $p = 4^0$

It can be observed approximately linear increase in lateral force F for each value of power P, and could approximate the family of linear functions useful $\mathbf{G_N}$-power applied force determining correspondence(Fig.10.). Example: - **P** = 95 [W] to maintain constant step $p = 4^0$ and = 2 mm is obtained with a linear function that can find value $\mathbf{G_N}$ lateral force **F** due to Coanda effect: Where do I noted the power of $\mathbf{P_C}$ fan beam intubated tail with index variable.

## 4. CONCLUSIONS

This study was conducted in the idea of highlighting the usefulness of the devices developing a force due to the Coanda effect.

To conclude, we may state the following:

1. For the same available energy $P_0$, the $D_f$ *force* gain may be obtained by decreasing the speed $V_D < V_M$ and increasing in the same time the ejected air flow.
2. In order to obtain the highest possible force for an available amount of energy, it is advisable to entrain into motion the highest fluid flow possible at a lower speed, instead of a small amount of fluid entrained into motion with a higher speed.
3. From the energetic point of view, for a helicopter, Coanda effect is a more efficient method than the tail rotor to obtain the lateral force needed to control the horizontal manoeuvrability and stabilizing in the same time the aerial platform created by a flying mono rotor helicopter.
4. The numerical results that were obtained are close enough to those we obtained through computational studies, taking into account the geometry of the tailboom and the fluid velocity inside the intubated tailboom rotor that generates the main carrier flow.
5. The study shows also a smooth growth index values $\mathbf{E_{fc}}$ for a sharp increase in force **F**, which requires to find an optimal position for the slot; this may be done with a pretty fair approximation of a helicopter (1:1 scale model).

## REFERENCES

[1] C. Berbente, N. V. Constantinescu, Dinamica gazelor şi Dinamica fluidelor vâscoase / Aerotermochimia, Bucureşti, UPB, 1985.
[2] E. Carafoli, N. V. Constantinescu, *Dinamica fluidelor compresibile*, Ed. Academiei R.S.R., Bucureşti,1981.
[3] H. Coanda, *Procédé de propulsion dans un fluide*, Brevet d'invention France, no. 762.688 /23.11.1932.
[4] H. Coanda, *Procédé et dispositif pour faire dévier une veine de fluide pénétrant dans un autre fluide*, Brevet d'invention France, no. 792.754 /08.10.1934.
[5] H. Coanda, *Perfectionnement aux propulseurs*, Brevet d'invention France, no. 796.843 /15.01.1935.
[6] R. J. Collins, *Aerial Flying Device* UK Patent Office no. GB 2,387,158 /08.10.2003.
[7] G. Hatton, S. McIntosh, GFS Projects Ltd., *Craft having flow-producing rotor and gyroscopic stability*, UK Patent Office no. GB 2,424,405 /23.03.2005.
[8] R. Van Horn James, McDonnel Douglas Co., *Circulation control slots in helicopter yaw control system*, US Patent, 4,948,069/12.05.1988.
[9] N. V. Constantinescu, S. Găletuşe, *Mecanica fluidelor şi elemente de aerodinamică*, Bucureşti , Ed. didactică şi pedagogică, 1983.
[10] S. Dinea, Teză de doctorat - *Contribuţii la studiul efectului Coandă*, Bucureşti, 2009.
[11] F. Nedelcuţ, *Current Aspects of Using Unmanned Aerial Vehicles in Environmental Monitoring*, The International Conference - Management and Sustainable Protection of Environment, 6-7 mai 2009, Alba-Iulia.
[12] I. Cîrciu, Teză de doctorat - *Îmbunătăţirea performanţelor de zbor ale elicopterelor prin aplicarea efectului Coandă - sistemul NOTAR*, Braşov, 2009.
[13] *** - *NEO - the new kit helicopter*, Retrieved on 25.04.2010, from http://www.youngcopter.com
[14] I. Cîrciu, F. Nedelcuţ, M. Boscoianu**,** *4th International Conference UAV World November 3 – 4, 2010, Frankfurt/Main, Germany.*